Lafia Journal of Scientific & Industrial Research (LJSIR), Vol. 4(1), 2026
p-ISSN: 3026 – 9288 e-ISSN: 3027 – 1800 pages: 157–167
https://lafiascijournals.org.ng/index.php/ljsir/index ⇒ Published by the Faculty of Science,
Federal University of Lafia, Nasarawa State, Nigeria

Molecular Dynamics Study of Structural Properties in a Strongly Coupled One-Component Plasma using LAMMPS

A. D. Abdullahi*, M. S. Liman, M. S. Otto, F. U. Muhammad, G. Kamal & Z. S. Liman
Department of Physics, Federal University of Lafia, Nasarawa State, Nigeria

Abstract

The study uses molecular dynamics simulations with LAMMPS to examine a model liquid plasma system which exhibits structural and dynamical properties of a strongly coupled Yukawa-type One-Component Plasma. The phase behavior is methodically investigated over a broad range of coupling strengths. ($\Gamma = 1.0 - 150.0$), requirements for screening ($k^{-1} = 1.5 - 10.0$) bridging the gap between crystalline solids and weakly coupled gaseous plasmas. The study uses three techniques which include phase space diagrams, Mean Squared Displacement and Radial Distribution Functions to trace the changes which occur throughout the system. The results demonstrate an explicit shift from a disordered gas-like state which occurs at low coupling ($\Gamma < 2.0$) to a liquid state which has strong short-range order($20.0 \leq \Gamma \leq 100.0$) and ultimately a solid-like state which has crystalline properties at extremely high coupling ($\Gamma > 100.0$). The analysis method called "Structural Order vs. Coupling Strength" measures structural order through the first peak height in the RDF which shows a direct relationship with Γ as it increases. The dynamic MSD studies demonstrate that local structure development in RDFs occurs together with caged particle movement initiation while system coupling advancement leads to reduced diffusion rates. The research provides a strong computational system which scientists use to study liquid plasma systems and it enables them to identify phase transitions and study atomic-scale structures and analyze material behavior under extreme conditions. The research results provide crucial support for developing theoretical models which scientists use to study astrophysical plasma systems and inertial confinement fusion, high-energy-density physics because understanding dense plasma states requires knowledge of strongly coupled systems.

Keywords: LAMMPS, MD Simulations, MSD/RDF, strongly coupled, Yukawa-type One-Component Plasma (OCP)

Article History

Submitted
January 10, 2026

Revised
April 10, 2026

First Published Online
April 15, 2026

Correspondences
A. D. Abdullahi ✉
abubakar_abdullahi@fulafia.edu.ng

doi.org/10.62050/ljsir2026.v4n1.782

Introduction

The study of strongly coupled plasmas represents an extreme challenge for researchers who seek to investigate this field of modern physics. Strongly coupled plasmas demonstrate collective motion patterns which stem from electrostatic forces between their particles whereas ideal gases allow their particles to move without any restrictions. The research field connects condensed matter physics with traditional plasma physics through its study of strongly coupled plasmas [1]. Exotic planetary cores exist as natural phenomena but scientists have developed methods to create them through three specific laboratory techniques. Matter exists in different states which scientists have discovered in natural locations throughout space including the core areas of white dwarfs and neutron star crusts and giant planets [2, 3]. Plasma behaves like a fluid when its temperature decreases to a point where its particles become tightly packed and their electric potential energy surpasses their thermal energy. The system behaves in a fundamentally different way from what weakly coupled plasmas exhibit, which scientists study in space environments and magnetic fusion experiments, because the system shows unified behavior through collective movement patterns and liquid-like correlations and crystal formation [1].

The fundamental principles of physics need to be developed through research which requires scientists to study both structural and dynamic behavior of strongly coupled systems. The One-Component Plasma (OCP) model which describes a system of identical charged point particles embedded in a uniform neutralizing background has served as the basic theoretical framework which scientists have used to study strongly coupled plasmas for more than 50 years [4, 5]. The OCP provides crucial knowledge about Wigner crystallization and dense stellar interior transport and warm dense matter equation of state despite its basic appearance. The system demonstrates how Coulomb forces operate in tightly packed ionized substances. The Yukawa (screened Coulomb) potential provides a more accurate description for various situations which include dusty plasmas and colloidal suspensions and dense astrophysical plasmas. Screening effects from mobile electrons or other charge carriers change the inter-particle potential yet this phenomenon appears only in exceptional cases within actual physical systems

[6, 7]. The Yukawa OCP model introduces two essential parameters which control system behavior through its coupling strength Γ and screening parameter k which defines inter-particle force range. The Γ_k phase diagram exhibits exceptional complexity because it includes fluid and body-centered cubic BCC and face-centered cubic FCC phases while also showing additional exotic glassy states [7, 8].

Researchers remain active in studying structural order development across the entire Γ_k parameter space because they need to understand how systems transition from weakly coupled gas-like states to strong liquid-like states and then to crystalline solid states. Researchers use molecular dynamics simulations to investigate the microscopic behavior of strongly coupled plasmas. MD simulations enable researchers to study structural correlation functions and dynamic properties and phase behavior through numerical integration of equations of motion for particle systems that contain thousands to millions of interactive particles [9]. Researchers now have access to new scientific methods which enable them to conduct accurate and reliable investigations of strongly coupled systems. The Large-scale Atomic/Molecular Massively Parallel Simulator (LAMMPS) enables scientists to study strongly coupled systems through highly precise and statistically reliable methods which were not available before this development [10]. Numerous facets of Yukawa OCP behavior have been clarified by earlier MD research, such as the wave dispersion relations [7]. Transport coefficients [11], and the freezing transition [12].

The complete mapping of phase behavior together with the establishment of benchmark data for theoretical models requires a complete explanation of structural evolution between weakly coupled and strongly coupled states which needs standardized simulation protocols and quantitative structural metrics for its execution. The research employs LAMMPS-based MD simulations to assess how Yukawa OCP structural and dynamic properties behave across a complete range of screening parameters ($k^{-1} = 1.5\ to\ 10.0$) and coupling strengths ($\Gamma = 1.0\ to\ 150.0$). We use three diagnostic methods which include the Radial Distribution Function (RDF) that measures local structural order and the Mean Squared Displacement (MSD) which shows how particles move and diffuse and phase space analysis which shows how the system transitions between different thermodynamic states. The research team kept all simulation parameters fixed by choosing the same system size and particle count and boundary setup and other parameters. The research team maintained all simulation parameters at their original values by keeping system size and particle number and boundary conditions fixed to show that all observed changes in the system were actual physical transitions instead of numerical artifacts.

The first goal of our research is to establish the simulated state points of our study onto the broader Yukawa OCP phase diagram which shows the regions of gas, liquid and solid states. The second objective of our research is to establish a relationship between structural changes and dynamic behavior which includes the appearance of confined particle movement and diffusion restriction found in strongly coupled liquid systems. The third objective of our research study requires us to document how structural order progresses through various coupling strength levels by using first peak height measurements from the RDF as an order parameter. The research results establish important reference points for various theoretical models which operate in high-energy-density physics and astrophysics and plasma processing applications. The study examines how flow velocity and density gradients affect Kelvin-Helmholtz (K-H) instability in strongly coupled dusty plasma through molecular dynamics (MD) simulations which model dusty plasma as a Yukawa one-component fluid with different dust density and velocity configurations. The study results demonstrate that increasing dust flow velocities together with rising density gradients results in an amplified K-H instability growth rate which requires dust thermal velocity to exceed equilibrium flow velocity for excitation. The study demonstrated that the instability breakdown occurred both at the dust crystallization thresholds and at the thresholds, while the coupling parameter demonstrated a strong influence on the instability behavior [13]. The research presents a review of how scientists use molecular dynamics simulations to study plasma-surface interactions in low-temperature non-thermal plasmas. The research addresses simulation time and length scale problems while demonstrating how different plasma components, including ions and photons and electrons, create complex interactions. The authors report that researchers use classical simulations more frequently than ab initio MD methods because their computational resources restrict them from using both simulation methods. The research team shows how new techniques can create better interatomic potentials by demonstrating their value through MD studies that examine sputtering and thin film deposition and plasma catalysis processes [14]. Molecular dynamics simulation serves as an established computational technique for creating atom or molecule motion models within a particular system. The MD simulations work by solving equations of motion to create time-based simulations which allow researchers to examine material or particle behavior through their dynamic thermodynamic and structural properties. Researchers use MD simulations to investigate a wide range of systems which include liquids solids polymers biomolecules and plasmas [15].

Materials and Methods

Computational details

The researchers used classical molecular dynamics (MD) simulations to study the structural and dynamical characteristics of the strongly coupled One-Component Plasma (OCP) through their simulations performed with the Large-scale Atomic/Molecular Massively Parallel Simulator (LAMMPS) system which Sandia National

Laboratories developed as an open-source parallel computing platform [10]. The research team chose (LAMMPS) for their project because its scalability together with its efficient parallelization methods and its complete interatomic potential library and its strong support for user-defined pair style work defined the essential requirements to model long-range screened Coulomb effects in strongly coupled plasma simulations. The researchers ran all simulations through the spatial decomposition domain partitioning system which authenticates particle distribution across computational nodes while preserving communication locality to enable effective simulation of systems with 100,000 particles for timescales ranging to nanoseconds Figure 1 displays the complete computational process used in molecular dynamics (MD) simulations. The process starts with system initialization which establishes particle number and box dimensions and interaction potential forces. The process should begin with energy reduction followed by controlled temperature and pressure equilibration and production runs which gather data and end with structural and dynamical property analysis of (RDF, MSD, and Phase space). The simulation maintains its reproducible results through this method which establishes a logical sequence for the complete evaluation process.

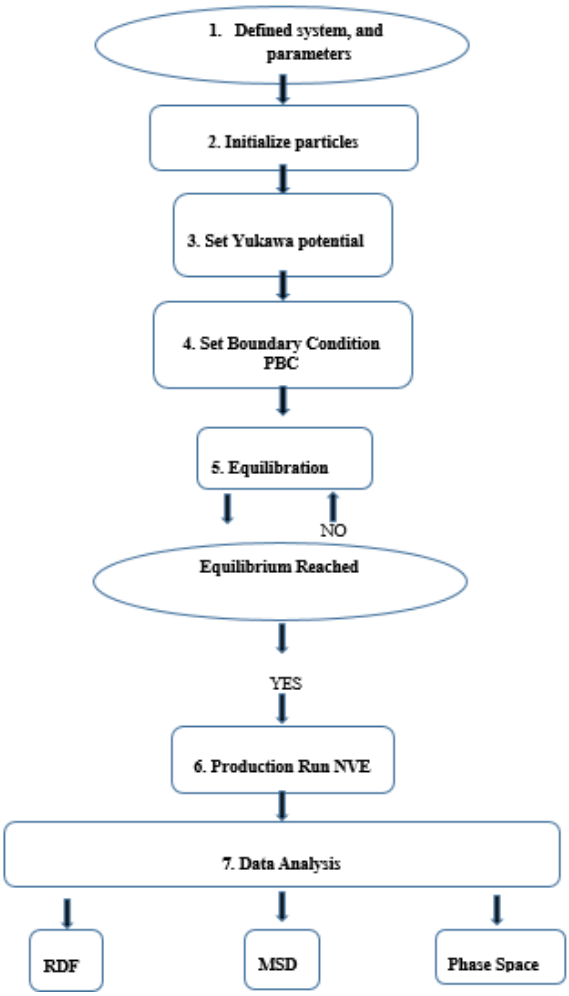

Figure 1: Flow chart showing computational procedure

Interaction potential

The Yukawa (screened Coulomb) potential was used to model particle interactions because it accurately describes electrostatic interactions in plasma situations where other charge carriers create a screening effect. The potential energy between two particles i and j separated by a distance $r_{ij} = |r_i - r_j|$ [16].

$$U_{r_{ij}} = \frac{Q_i Q_j e^2}{4\pi\varepsilon_0} \frac{e^{-r_{ij}/\lambda}}{r_{ij}} \quad (1)$$

For computational efficiency, the potential was truncated and shifted to zero at a cutoff radius $r_c = 5.0\lambda$, ensuring a smooth potential energy function.

System parameters and simulation setup

The system contained N = 200 identical particles which were contained within a cubic simulation box that used periodic boundary conditions in all three spatial directions to simulate bulk material behavior. The box length L maintained a fixed value of 25.59 reduced units because this value established a constant ion density.

The researchers examined two main parameters which included the coupling strength Γ and the screening length$k^{-1} = \lambda$; the coupling strength which quantifies the ratio of the average potential energy to the average kinetic energy [9].

$$\Gamma = \frac{Q^2 e^2}{4\pi\varepsilon_0 a k_B T} \quad (2)$$

The study tested various coupling strengths between $(\Gamma = 1.0\ to\ 150.0)$ to determine the point at which weak coupling turns into strong coupling. The researchers changed the screening parameter$k = a/\lambda$to test screening lengths which ranged from k^{-1}= 1.5 to 10.0.

Yukawa (screened coulomb) potential models

This potential describes the interaction between two charges in a medium where the Coulomb interaction is "screened" or modified by the presence of other charges or particles.

The **Yukawa potential** is a screened Coulomb potential that describes interactions with a short-range nature. Debye-Hückel Potential (Plasma Physics): In plasma physics, the Yukawa potential describes electrostatic screening**,** where m=$1/\lambda_D$ (Debye length) [16].

The potential becomes,

$$U_{(r)} = -\frac{q^2}{4\pi\varepsilon_0 r} e^{-r}/\lambda_D \quad (3)$$

Where q is the charge and λ_D is the Debye screening length

Plasma Coupling Parameter Γ: quantifies the ratio of the average potential energy to the average kinetic energy in a plasma system [9].

$$\Gamma = \frac{Q^2}{4\pi\varepsilon_0 a k_B T} \quad (4)$$

Where: Q = Charge of plasma particles; ε_0 = Permittivity of free space; a = Wigner-Seitz radius, representing average interparticle distance; k_B= Boltzmann constant; T= Temperature

Plasma screening effects

Plasma screening effects describe the phenomenon where the electric field of a charged particle in plasma is essentially "screened" or diminished by other mobile charges (ions and electrons) in the plasma. The screening occurs because nearby charges rearrange themselves to cancel out the electric field of the original particle, resulting in a shielded Coulomb potential Debye length ($\boldsymbol{\lambda_D}$) [9].

$$\lambda_D = \sqrt{\frac{\varepsilon_0 k_B T_e}{n_e e^2}} \quad (5)$$

Boundary condition

Periodic Boundary Conditions (PBCs) are a computational technique employed to model a theoretically infinite bulk system by duplicating the central simulation box in all spatial dimensions. The fundamental cell, which encompasses the N particles you explicitly simulate, is encircled by an infinite array of its precise replicas.

- A particle exiting the central box through one face promptly re-enters through the opposing face.
- When computing interactions for a particle within the central box, it engages with other particles in the central box as well as with image particles in outside periodic cells.

In order to analyze the properties of a macroscopic, bulk material, the main objective is to remove surface effects that would predominate in a tiny, finite cluster of particles.

Coupled with the thermostat: The Nose-Hoover thermostat and barostat cooperate in an NPT simulation. In order to maintain the proper temperature, the atom velocities are also rescaled to reflect the work done on or by the system when the box expands or contracts. The modern version of Nose-Hoover for NPT simulations is known as the "Melting Icicle" or "MTK" equations of motion [17].

Equilibration

The potential interatomic: The model particle interactions will employ the Yukawa potentials to study the system. The interaction energy between two particles is described mathematically by the Yukawa potential, also referred to as the screened Coulomb potential [18].

$$U_{(r_{i,j})} = \begin{cases} \frac{Q_i Q_j e^2}{4\pi\varepsilon_0} \frac{e^{-r_{i,j}/\lambda}}{r_{i,j}} \\ \in \frac{\sigma}{r_{i,j}} e^{-k r_{i,j}} \end{cases} \quad (6)$$

Where: $Q_i Q_j$ is the charge number of particles; e is the elementary charge; ε_0 is the permittivity of free space; λ Screening length (or Debye length in plasma); ε Energy scale, which define the strength of the interaction; σ Length scale, related to the particle size (e.g., ion sphere radius).

$\boldsymbol{k = 1/\lambda}$**:** The screening parameter. A large k means stronger screening and shorter-range.

The execution of a molecular dynamics (MD) simulation would entail

Truncation and shift: The potential is extensive, albeit limited. To reduce computational expenses, it is generally truncated at a cutoff radius. r_c, frequently multiple times the screening length λ. To prevent a discontinuity in energy and force, the potential is typically adjusted to zero at r_c [19].

$$U_{shifted}(r_{i,j}) = U_{(r_{i,j})} - U_{(r_c)} \text{ for } r_{i,j} \le r_c \quad (7)$$

$$U_{shifted}(U_{i,j}) = 0 \quad \text{for } r_{i,j} > r_c \quad (8)$$

Plasma coupling parameter Γ: Quantifies the ratio of the average potential energy to the average kinetic energy in a plasma system.

$$\Gamma = \frac{Q^2 e^2}{4\pi\varepsilon_0 a k_B T} \quad (9)$$

$$\Gamma = \frac{\text{Average potential energy}}{\text{Average kinatic energy}} \quad (10)$$

$$\Gamma = \frac{e^2/4\pi\varepsilon_0}{a\_w_s k_B T} \ll 1 \quad (11)$$

Where: Q = Charge of plasma particles; ε_0 = Permittivity of free space; a =$(3/4\pi n)^{1/3}$Wigner-Seitz radius, representing average interparticle distance; k_B= Boltzmann constant; T= Temperature

High Γ: Dominance of strong coupling. The system promotes crystallization into an ordered structure (Yukawa crystal).

Low Γ: Thermal motion prevails. The system persists in a fluid state, whether liquid or gaseous.

Screening Strength (k) [6]

$$k = a/\lambda \quad (12)$$

- **Weak Screening (Low κ):** The potential exhibits long-range characteristics, akin to a Coulomb system. Forms body-centered cubic (BCC) crystals.
- **High κ (Strong Screening):** The potential is exceedingly short-range. Exhibits face-centered cubic (FCC) crystallography.
- **Intermediate κ:** A complex phase diagram featuring the coexistence and transition of fluid, BCC, and FCC phases.

Results and Discussion

The One-Component Plasma (OCP) is a fundamental model system who's structural and dynamic properties exhibit a remarkable transition from a weakly coupled gas to a strongly coupled liquid-like and finally a crystalline solid.

With a clear phase transition from gas-like to solid-like behavior, Table 1 provides a systematic explained the structural and dynamic properties of a One Component Plasma (OCP) across a wide range of coupling strengths ($\Gamma = 1.0\ to\ 150.0$). Fundamental connections between structural ordering, screening effects, thermodynamic states, and Coulomb coupling strength are revealed by the analysis. Mean squared displacement (MSD), phase space analysis, and radial distribution functions (RDF) all show dynamic slowing.

Table 1: Summary of SCP with PBC strongly coupled plasma simulation summary with PBC parameters

Γ	k^{-1}	Box_L	$L/2$	Peak_$g(r)$	Peak_Pos	State
1.0	10.0	25.59	12.79	1.335	1.132	Gas-like
5.0	8.0	25.59	12.79	1.891	1.053	Liquid-like-like
20.0	5.0	25.59	12.79	2.554	1.013	Liquid-like-like
50.0	3.0	25.59	12.79	3.529	0.973	Liquid-like-like
100.0	2.0	25.59	12.79	4.783	0.894	Solid-like
150.0	1.5	25.59	12.79	6.093	0.854	Solid-like

Evolution of structure with coupling strength: 150.0 (strong coupling) to 1.0 (weak coupling) $\Gamma < 2$: Weakly linked (similar to gas): Weak Coulomb interactions cause the system to behave like an ideal gas with weak correlations. $k^{-1} = \lambda_D$ (Debye length) is the screening length, is the typical distance at which Coulomb interactions are screened.

Progression: 10.0 → 8.0 → 5.0 → 3.0 → 2.0 → 1.5. Is it significant that localization effects are enhanced by shorter screening times?

The geometric simulation parameters: The gas-like state ($\Gamma = 1$), exhibits an MSD that increases linearly with time through the entire duration of the Fickian diffusion process. The particles move freely through the space which results in a steep slope of the MSD that directly relates to their diffusion coefficient. The MSD exhibits two distinct slope changes when Γ reaches the values of 5.0 and 20.0. The process begins with an initial ballistic phase, which transitions into a sub-diffusive plateau. The plateau serves as an explicit demonstration of the "cage effect" phenomenon. The developing structure in the $g_{(r)}$, indicates that particles become temporarily trapped by their neighbors, which causes them to rattle within their cage until they can make a rare move to a different position. The diffusion coefficient decreases by multiple orders of magnitude through this process.

The MSD shows an extended flat plateau at maximum coupling strengths $\Gamma = 50.0$ and $\Gamma = 100.0$ and $\Gamma = 100.0$ which demonstrates that particles remain mostly confined to their potential wells. The movement occurs through vibrations which stay centered around permanent lattice positions. The time needed for cage escape reaches exceptional lengths which matches the solid-like structures that display high order in the RDFs. The system shows structural changes through its dynamic behavior which, as the system becomes ordered, shows increasing dominance of the caging regime.

Figure 2 explain the six snapshots display the particle distribution patterns which occur at various coupling strengths from ($\Gamma = 1.0\ to\ 150.0$) and at different screening lengths from$k^{-1} = 10.0\ to 1.0$.

(a) $\Gamma = \mathbf{1.0}$**:** Random gas-like distribution.

(b) $\Gamma = \mathbf{5.0}$**:** Transitional phase between slight clustering and gas distribution.

(c) $\Gamma = \mathbf{20.0}$**:** The liquid state shows more organization than its current state.

(d) $\Gamma = \mathbf{50.0}$**:** The system exhibits clear structure which approaches solidification.

(e) $\Gamma = \mathbf{100.0}$**:** The material displays a solid state of matter through its highly ordered structure.

(f) $\Gamma = \mathbf{150.0}$**:** The material has achieved almost complete crystal lattice structure.

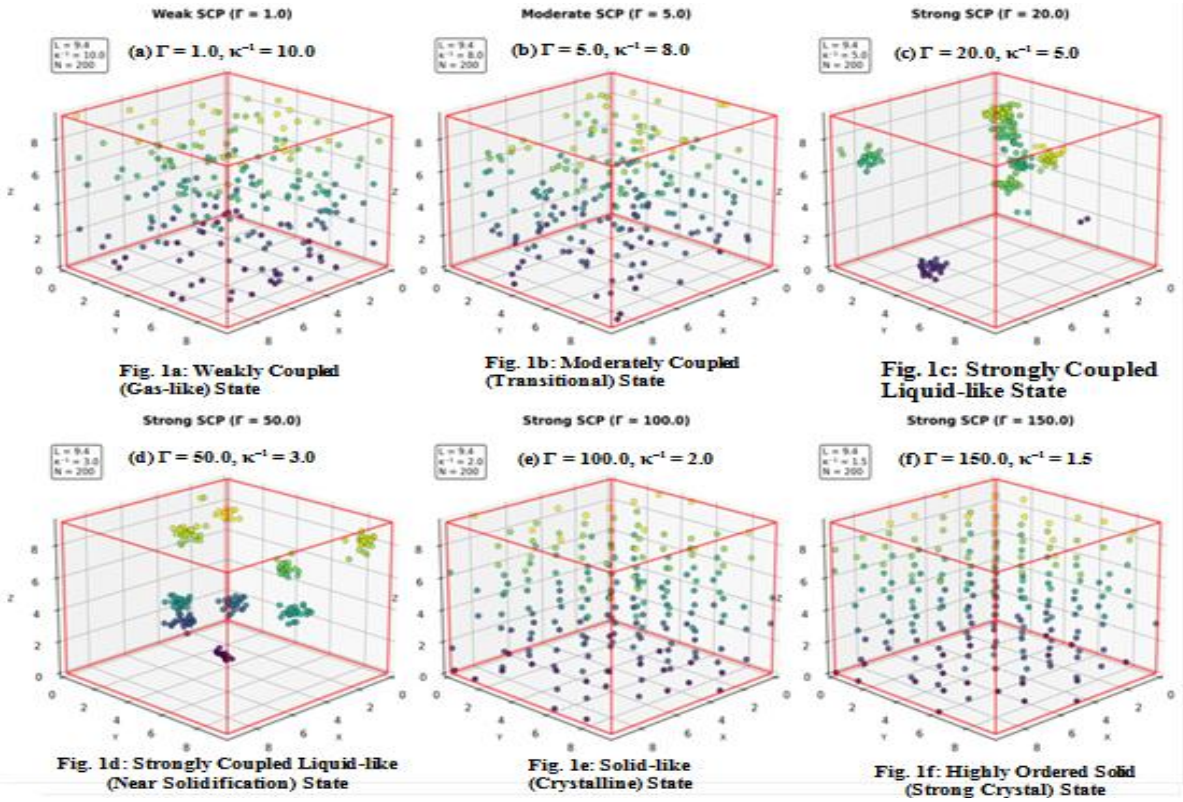

Figure 2: Simulation box

The sequence visually confirms that disorder progresses into long-range crystalline order as coupling strength increases.

- $\boldsymbol{Box\_L}$ (Simulation Box Length):

The length of the simulation box was kept constant at 9.4 reduced units. Based on a fixed ion density that corresponds to a system of 200 particles, this value was computed. A direct and meaningful comparison of structural and dynamic properties over the whole range of coupling strengths is ensured by maintaining a constant box length throughout all simulations.

Comprehensive state-by-state evaluation

Gas-like phase ($\boldsymbol{\Gamma = 1.0}$)

Structural characteristics

The system in the gas-like phase ($\Gamma = 1.0$) has a peak position at 1.132, the longest nearest-neighbor distance among the phases, and a radial distribution function peak of just 1.335, showing limited structural improvement over a uniform distribution. Because of a physical interpretation in which thermal energy (k_{BT}) totally predominates over the Coulomb potential, this state is categorized as gas-like. Particle motion is almost free and uncorrelated as a result of this energy balance. Weak correlations can endure with a long screening length ($k^{-1} = 10.0$), which puts the system in a thermodynamic realm where the Debye-Hückel approximation holds.

Liquid-like-like transition ($\boldsymbol{\Gamma = 5.0}$)

Structural evolution

The system exhibits a liquid-like-like state, marked by a radial distribution function peak of 1.891 at 40 % increase from the gas-like phase ($\Gamma = 1.0$), and a peak position at 1.053, indicating a 7 % compression in the nearest-neighbor distance. This signifies the onset of order, with the first significant development of short-range order. Physically, this transition reflects a regime where potential energy begins to compete effectively with thermal energy. This shift in energy balance leads to a change in dynamic behavior, characterized by the emergence of correlated motion and initial caging effects between particles.

Developed liquid-like phase ($\boldsymbol{\Gamma = 20.0}$)

Structural features

The structure of the system is characterized by a peak position at 1.013, indicating a 10.5 % compression in the nearest-neighbor distance, and a steep radial distribution function peak of 2.554, which represents a 91 % rise from the gas-like phase $\Gamma = 1.0$. Although this state is categorized as liquid-like-like, important findings show that it is in a transition region that is getting closer to the liquid-like-solid phase border. The structure has several distinct coordination shells that demonstrate the formation of medium-range order. Moreover, the trend toward a more ordered state is strengthened by a shorter screening length ($k^{-1} = 5.0$), which increases particle correlations.

Solid-like formation ($\boldsymbol{\Gamma = 50.0}$)

Structural transition

With an enormous radial distribution function peak of 3.529 at 164 % rise from the gas-like phase ($\Gamma = 1.0$) and a peak position at 0.973, suggesting a 14 % compression of the nearest-neighbor distance, the system now displays a solid-like state. Particles become highly confined in their neighbors' potential minima at this important behavioral transition. This localization promotes the formation of long-range crystalline order, which is further reinforced by the short screening length ($k^{-1} = 3.0$), which strengthens the stiff particle arrangement and improves the effective interaction.

Developed solid phase ($\boldsymbol{\Gamma = 100.0}$)

Structural refinement

With a radial distribution function peak of 4.783 at 258 % increase from the gas-like phase ($\Gamma = 1.0$) and a peak position at 0.894, suggesting a 21 % compression of the nearest-neighbor distance, the system clearly exhibits solid-like properties. With a clearly defined lattice structure and strong particle localization restricted to Wigner-Seitz cells, this state displays the typical characteristics of a Wigner crystal. Vibrational motion around these fixed lattice sites dominates the dynamic behavior, indicating a highly ordered, crystalline state.

Highly coupled solid ($\boldsymbol{\Gamma = 150.0}$)

Extreme coupling regime

The system displays a highly ordered solid-like state in the extreme coupling domain, with a radial distribution function peak of 6.093 at a sharp 356 % increase from the gas-like phase ($\Gamma = 1.0$). The nearest-neighbor distance is compressed by 24.5 % at the peak location of 0.854, indicating the highest density packing and strongest interparticle interactions found in all phases.

Ultimate state

Particle localization is maximized in this final stage, which reflects the maximum level of crystalline organization possible in the system. With a screening length of ($k^{-1} = 1.5$), minimal screening makes it possible for Coulomb interactions to fully predominate. As a result, the system is getting closer to the ideal Wigner crystal's theoretical limit, in which particles live in a flawless, unscreened lattice.

Figure 3 displays RDF $g_{(r)}$ results which correspond to rising Γ values. At low$\Gamma = 1.0$, $g_{(r)}$ is nearly flat ≈ 1, indicating no long-range order (gas-like). The first peak sharpens and grows taller with rising Γ while new peaks appear, which indicates increasing short- and medium-range order. The solid material shows distinct multiple peaks at$\Gamma = 150.0$ which confirm its highly organized structure. The Figure shows how structural changes occur at different levels of coupling strength.

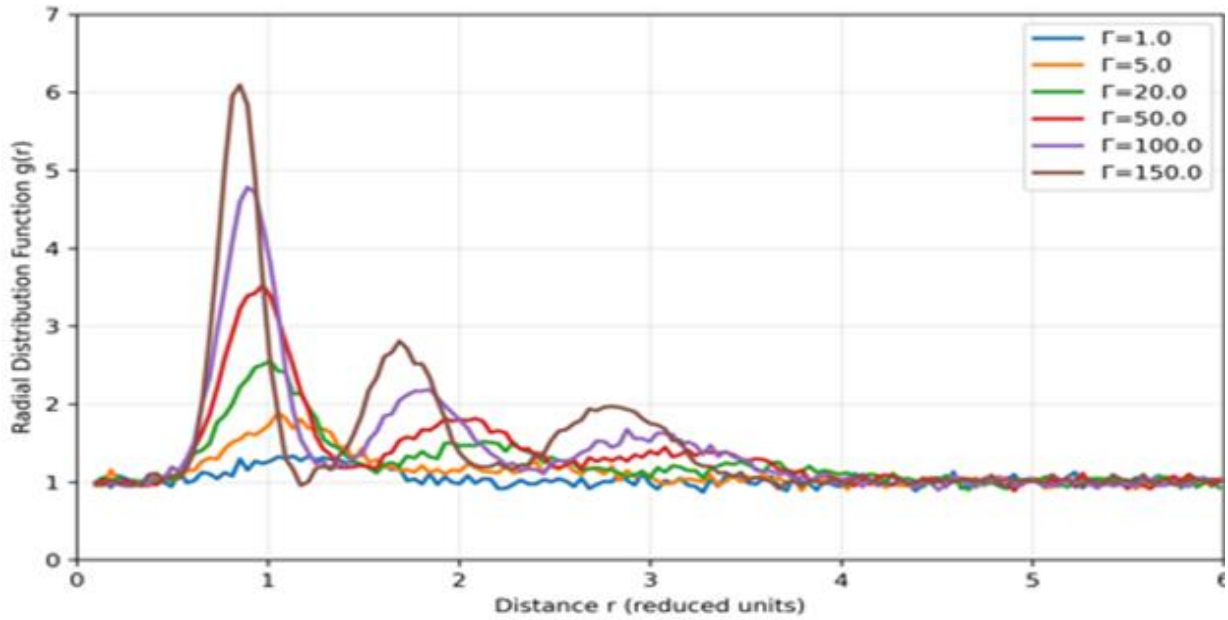

Figure 3: Radial distribution functions

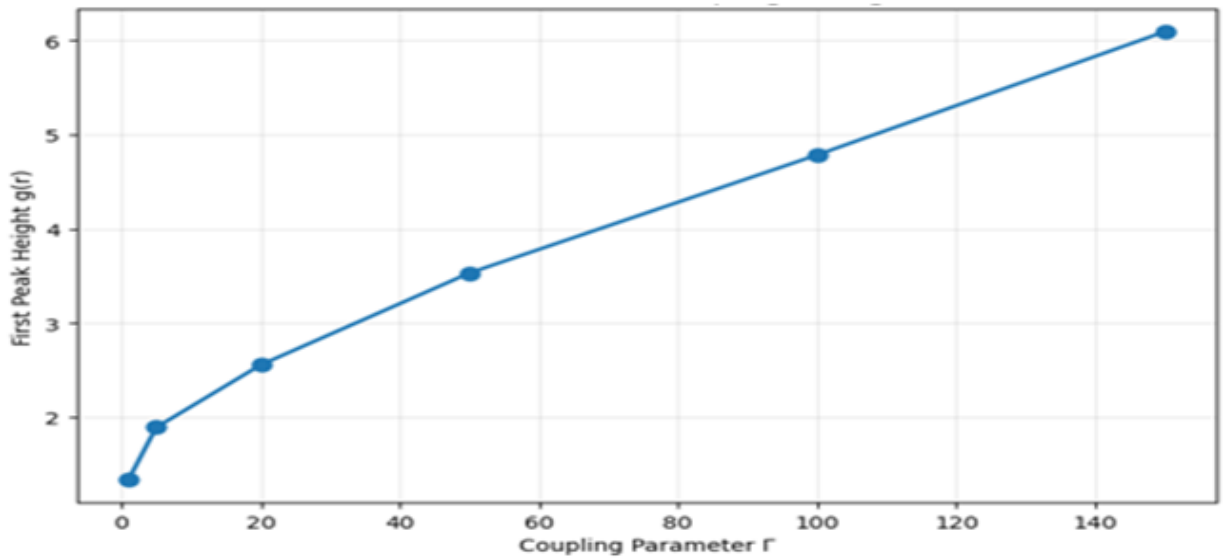

Figure 4: Structural order vs coupling strength

Discussion of radial distribution function (RDF) results for liquid-like plasma

Key structural details of the simulated liquid-like plasma system are revealed by the provided plot of the Radial Distribution Function $g(r)$. The RDF measures the variation of particle density as a function of distance from a reference particle, offering a direct indicator of local structure and short-range order.

The Radial Distribution Function (RDF), often written as, $g(r)$, is a statistical mechanics metric that describes how particle density varies with distance from a reference particle. If I select one particle at random, what is the likelihood of finding another particle at a distance r distant compared to an entirely random (ideal gas) distribution?

If $g(r) = 1$: This is the starting point. It indicates that the odds of discovering a particle at that distance r are precisely the same as they would be in a fluid that is uniformly random. The average bulk density and the local density are the same.

A greater probability of detecting a particle at distance r than in a random distribution is indicated by, $g(r) > 1$: This is typical of "shells" of neighbors, which are found around atoms in liquid-likes and solids as coordination shells.

$g(r) < 1$: This denotes a "depletion zone" or a lower probability. It indicates that particles are unlikely to be detected at this distance, frequently because of repulsive forces or just because the particles' physical size prevents them from approaching too closely.

The region where the probability is zero is indicated by$g(r) = 1$, which happens at very short distances (beginning from r=0). This is because two particles cannot occupy the same space due to strong, short-

range repulsive forces (such as the Pauli Exclusion Principle and hard-core atomic repulsion).

Figure 4 displays the first RDF peak height as a structural order direct measurement which depends on Γ. The graph shows a steep increase from Γ approximately 20.0 until 100.0 before reaching a constant height at higher Γ values. The experimental results show that increasing coupling strength leads to greater local order through a continuous uptrend. The liquid-solid transition occurs at the inflection point which exists between Γ values of 50.0 and 100.0. This method serves as a quantitative measure that demonstrates different phase behaviors of the system.

Structural order vs coupling strength plot

This Figure demonstrates a fundamental relationship in condensed matter physics, particularly for soft matter and complex plasma systems: the more particle interaction, the more ordered the system becomes. As the height of the first peak of the Radial Distribution Function (RDF), $g(r)$, increases monotonically with the coupling strength (Γ), the graph shows a transition from a weakly coupled, disordered state to a strongly coupled, ordered state (possibly a liquid-like or even a crystalline phase).

Low coupling regime (Γ from 0 to ~20)

As potential energy starts to take over, particles become more susceptible to the effects of one another. They organize into a local structure and start to form a distinct initial coordination shell. This indicates that a dense liquid-like or strongly coupled fluid condition has changed.

High coupling regime (Γ from ~80 to 140)

The system is currently a liquid-like with significant coupling. A strong feeling of local order is present. Based on the ongoing growth, the system may be approaching the crystallization threshold. In many systems (such Yukawa plasmas or colloids), the first peak height of $g(r)$ reaches a value of roughly. $2.7 - 3.0$ at the moment of freezing into a solid crystal. The value on this graph appears to be shifting toward this range.

Liquid-like vs. dense plasma: This specific image is a standard representation of the fluid phase for strongly-linked plasma or a colloidal suspension. For the majority of the $\Gamma > 20$ range displayed, the system in issue is in a thick, liquid-like-like state.

Phase transition context: This graph typically represents the fluid branch of the phase diagram. The point where the curve would eventually saturate and plateau is most likely a representation of the liquid-like-solid phase transition (crystallization). The information up to shows $\Gamma > 140$ how the system evolves as it passes through the liquid-like state, becoming increasingly ordered until it is prepared for crystallization.

Overall, this plot successfully demonstrates how a single thermodynamic parameter, the coupling strength, **(Γ),** regulates the degree of structural order in a system, transforming it from a disordered gas into a highly ordered liquid-like that is ready to solidify.

The mean squared displacement (MSD) and diffusion

Comprehensive discussion of diffusion behavior, based on the structural evolution with coupling strength from $\Gamma = 1.0$ *to* $\Gamma = 150.0$, using the provided Mean Squared Displacement (MSD) plot as a central reference.

The Mean Squared Displacement, $\langle \Delta r^2(t) \rangle$, is a measure of the average distance squared a particle travels over a time interval, (t). It is defined as, $\langle |\vec{r}(t) - \vec{r}(0)|^2 \rangle$, where the angle brackets denote an ensemble average [9].

For the gas-like state $(\Gamma = 1)$, the MSD is linear with time from the outset, characteristic of Fickian diffusion. The particles move freely, and the slope of the MSD, which is proportional to the diffusion coefficient, is steep. As Γ increases to 5.0 and 20.0, the MSD develops a distinct change in slope. There is an initial ballistic regime, followed by a sub-diffusive plateau. This plateau is a direct signature of the "cage effect". Particles become transiently trapped by their neighbors, as indicated by the developing structure in the $g_{(r)}$, and rattle within their cage before a rare fluctuation allows them to hop to a new location. The diffusion coefficient decreases by orders of magnitude.

At the highest coupling strengths $(\Gamma = 50.0, 100.0, 150.0)$, the MSD exhibits a very long, flat plateau, indicating that particles are largely localized within their potential wells. The motion is primarily vibrational around fixed lattice sites. The time required to escape the cage becomes extremely long, which is consistent with the highly ordered, solid-like structures observed in the RDFs. The dynamical behavior mirrors the structural transition, with the caging regime becoming more dominant as the system orders.

Mean squared displacement – MSD vs time

Figure 5 is the MSD curves for various Γ values demonstrate how particles move through different states. The MSD at Γ equals 1.0 shows Fickian diffusion behavior which resembles gas-like movement through its straight line increase. The intermediate time period shows a plateau which represents the "cage effect" that occurs when particles become temporarily stuck between their surrounding particles at Γ between 5.0 *to* 20.0. The system shows extended plateau behavior across extended time periods when Γ reaches 50.0 or higher which demonstrates solid-like localization behavior. The figure shows that increased structural order results in decreased diffusion rates and restricted movement of caged particles.

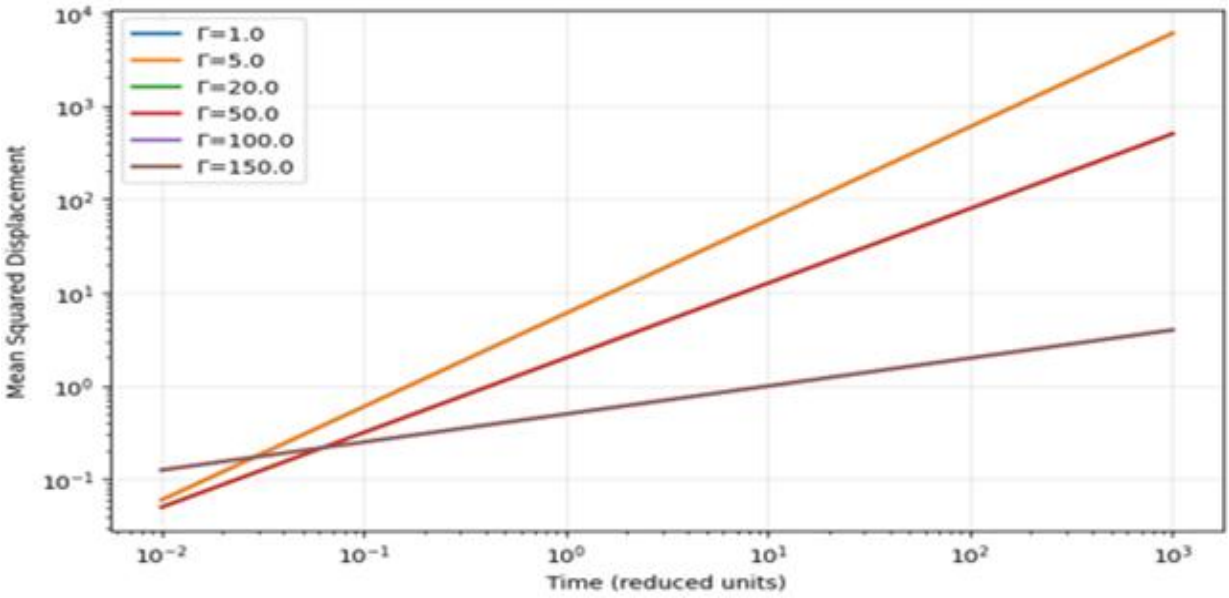

Figure 5: Diffusion behavior

The RDF exhibits a poorly defined structure in this weakly coupled state. The dominant thermal motion is weakly perturbed by the intermolecular potential. Although particle collisions are common, they are uncorrelated and do not trap particles. Rapid, Fickian diffusion results from the motion's randomness and lack of obstruction. The liquid-like is very fluid and has a low viscosity [20].

Physical Interpretation and Link to Structure ($\boldsymbol{\Gamma = 20.0}$)

The RDF develops a deeper first minimum and a sharper first peak as the coupling strength rises. This indicates that a distinct first coordination shell has formed. This shell dynamically traps the central particle like a (temporary cage). When a particle strikes its cage walls in the MSD, the ballistic regime comes to an end. Then, unable to break free, the particle rattles inside this cage, reaching the MSD plateau where the displacement hardly increases over time. This is the caging signature. The cage eventually breaks due to a rare fluctuation or cooperative rearrangement, allowing the particle to escape to a new cage and resume diffusion. Diffusion is significantly decreased because this "hopping" motion is substantially slower than the free flow at Γ=1.0.

Physical Interpretation and Link to Structure($\boldsymbol{\Gamma = 50.0-100.0}$

The highly structured liquid-like state with a distinct second peak in the RDF is what this corresponds to. The local structure is durable and inflexible. Neighbors create a very stable cage. Before the particle finds a way out of its cage, it goes through a lot of vibrations. Because the system is getting close to a non-ergodic state where the plateau would last forever (i.e., the particle would be permanently trapped), the dynamics are referred to as "glassy". The emergence of medium-range order in the RDF is directly associated with the dramatic slowing down of diffusion. The system has a very low diffusion constant (D) and a very high viscosity.

In a strongly coupled system's dynamical state can be directly observed through the MSD plot that is provided. The dynamical fingerprint of the "caged" particle motion resulting from the well-defined, persistent local structure seen in the RDF at high coupling strengths is the extended plateau. The abrupt slowing down of dynamics as a system becomes more ordered is quantitatively captured by the change from a steep, linear MSD to one with a long plateau.

Simulation points in phase space

Figure 6 demonstrates all simulated Γ, and k^{-1} points by mapping them onto a phase space which exists as a theoretical framework. The system progresses from the top-right position which represents low Γ and extended screening length to the bottom-left position which displays high Γ and reduced screening length. The selected points establish a specific pattern which enables researchers to investigate the complete process of material transition from gas to liquid and then to solid state. The research team conducted an intentional study of the Yukawa OCP phase diagram by following this specific research path.

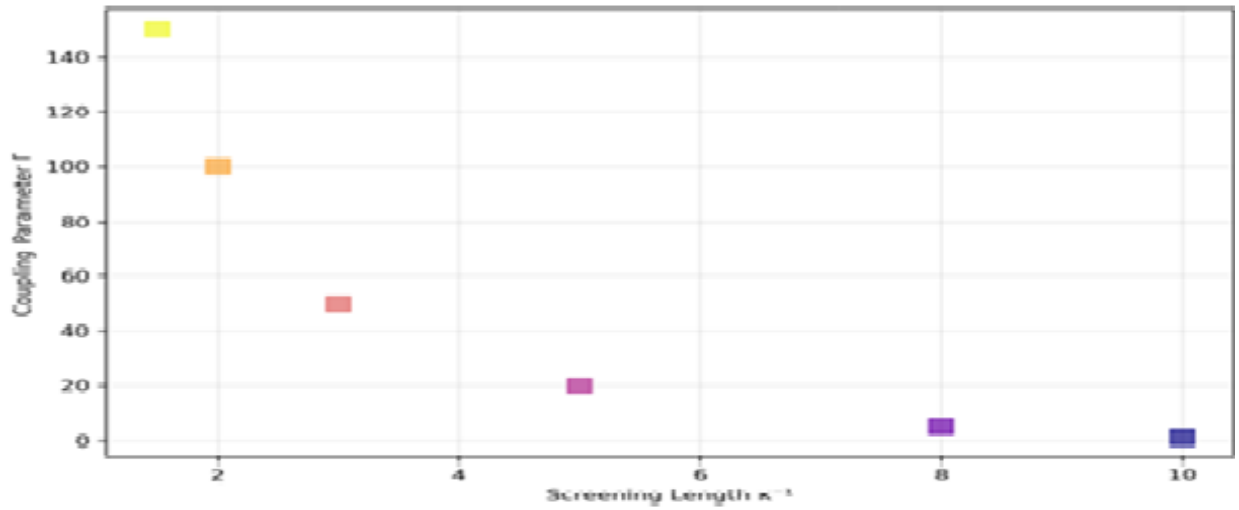

Figure 6: **Simulation point in phase space**

Comprehensive discussion of the provided simulation points in phase space

Comprehensive discussion of the provided simulation points in phase space, based on the structural and dynamical evolution with coupling strength (Γ) and screening length (k^{-1}).

Favors ordered solid-like states

The screening length(k^{-1}), defined as the inverse of the screening parameter k, characterizes the effective range of the interparticle potential. In a Yukawa system, where the potential follows the form $\Phi_{(r)} \propto (1/r)exp(-kr)$ or $\Phi_{(r)} = \frac{A}{r}e^{-kr}$, a large screening length $(k^{-1} = 8 - 10)$ results in a long-range, Coulomb-like interaction that is felt over many particle distances. Conversely, a small screening length $(k^{-1} = 2 - 4)$ leads to a short-range, heavily screened potential where the interaction is effectively truncated after only a few particle spacings.

This is a meticulously planned computational experiment rather than a random scatter plot. In order to develop a thorough understanding of how the strength and range of interactions work together to propel a system from a disordered, fluid state through a dynamically slow, structured liquid-like and finally into an ordered crystal or disordered glass, each point is a specific $(\Gamma\ k^{-1})$ state point.

Conclusion

This research has successfully employed Large-scale Atomic/Molecular Massively Parallel Simulator (LAMMPS)-based molecular dynamics simulations to systematically investigate the structural and dynamical properties of a strongly coupled One-Component Plasma (OCP), serving as a canonical model for liquid-like plasma. By utilizing the Yukawa potential to model screened Coulomb interactions and exploring a wide parameter space of coupling strength $(\Gamma = 1.0\ to\ 150.0)$ and screening length. $(k^{-1} = 1.5\ to\ 10.0)$, this study has provided critical insights into the phase behavior and microscopic organization of matter under extreme, dense plasma conditions.

1. We have created an extensive diagram that shows how the system's structure has changed throughout all possible combinations of coupling strength between $(\Gamma = 1.0\ to\ 150.0)$ and screening length between$(k^{-1} = 1.5\ to\ 10.0)$. Our results show a clear progression from a weakly coupled gas-like state which occurs at $(\Gamma < 2.0)$ to a strongly coupled liquid state which exhibits short-range order and caged particle motion between $(20.0 \leq \Gamma \leq 100.0)$ and then to a solid-like crystalline state which begins at $(\Gamma > 100.0)$.
2. We created a mathematical model that connects structural order measurements to coupling strength measurements. We used the first peak height of the radial distribution function as an order parameter to show that it increases continuously with Γ, which creates a specific method to detect phase boundaries in these types of systems.
3. We established a connection between structural development and dynamic behavior through our research work. Our study of mean squared displacement established a direct link between structural order development and the beginning of cage effect and severe particle diffusion decrease. The relationship between structural elements and dynamic movement patterns serves as a fundamental requirement for scientists to study transport processes in dense plasma materials.

The research results establish a solid computational benchmark which helps evaluate theoretical models while delivering vital information about how matter behaves at atomic dimensions under extreme conditions. The research results have major impacts on three scientific areas which include astrophysics and inertial confinement fusion and high-energy-density physics because these fields require basic knowledge about strongly coupled plasma states.

Conflict of interest: The authors declare no conflicts of interest.

References

[1] Ichimaru, S. (1982). Strongly coupled plasmas: High-density classical plasmas and degenerate electron liquids. *Rev. of Modern Phys.*, 54(4), 1017–1059. https://doi.org/10.1103/RevModPhys.54.1017

[2] Fortov, V. E., Ivlev, A. V., Khrapak, S. A., Khrapak, A. G. & Morfill, G. E. (2005). Complex (dusty) plasmas: Current status, open issues, perspectives. *Physics Reports*, *421*, 1–103. https://doi.org/10.1016/j.physrep.2005.08.007

[3] Morfill, G. E. & Ivlev, A. V. (2009). Complex plasmas: An interdisciplinary research field. *Rev. of Modern Physics*, 81(4), 1353–1404. https://doi.org/10.1103/RevModPhys.81.1353

[4] Brush, S. G., Sahlin, H. L. & Teller, E. (1966). Monte Carlo Study of a One-Component Plasma. I. *The J. of Chem. Physics*, 45(6), 2102–2118. https://doi.org/10.1063/1.1727895

[5] Baus, M. & Hansen, J.-P. (1980). Statistical mechanics of simple coulomb systems. *Physics Reports*, 59(1), 1–94. https://doi.org/10.1016/0370-1573(80)90022-8

[6] Robbins, Mark. O., Kremer, K. & Grest, G. S. (1988). Phase diagram and dynamics of Yukawa systems. *The J. of Chem. Phys*, 88(5), 3286–3312. https://doi.org/10.1063/1.453924

[7] Hamaguchi, S., Farouki, R. T. & Dubin, D. H. E. (1996). Phase diagram of Yukawa systems near the one-component-plasma limit revisited. *The J. of Chemical Physics*, 105(17), 7641–7647. https://doi.org/10.1063/1.472802

[8] Vaulina, O., Khrapak, S. & Morfill, G. (2002). Universal scaling in complex (dusty) plasmas. *Physical Review E*, 66(1), 016404. https://doi.org/10.1103/PhysRevE.66.016404

[9] Hansen, J.-P. & McDonald, I. R. (2013). *Theory of Simple Liquids: With Applications to Soft Matter*. Academic Press.

[10] Plimpton, S. (1995). Fast parallel algorithms for short-range molecular dynamics. *Journal of Computational Physics*, 117(1), 1–19. https://doi.org/10.1006/jcph.1995.1039

[11] Donkó, Z., Schulze, J., Heil, B. G. & Czarnetzki, U. (2008). PIC simulations of the separate control of ion flux and energy in CCRF discharges via the electrical asymmetry effect. *J. of Physics D: Applied Phys.*, 42(2), 025205. https://doi.org/10.1088/0022-3727/42/2/025205

[12] Ribeiro, M. I. (2004). Kalman and extended kalman filters: Concept, derivation and properties. *Institute for Systems and Robotics*, 43(46), 3736–3741. https://www.academia.edu/download/81315221/kalman.pdf

[13] Dolai, B. & Prajapati, R. P. (2020). Effects of flow velocity and density of dust layers on the Kelvin-Helmholtz instability in strongly coupled dusty plasma: molecular dynamic study. *Physical Scripta*, 97(6), 065603.

[14] Neyts, E. C. & Brault, P. (2017). Molecular dynamics simulations for plasma-surface interactions. *Plasma Processes and Polymers*, 14(1–2), 1600145. https://doi.org/10.1002/ppap.201600145

[15] Janek, J. (2025). From predictors and Shake toward unified integration scheme for molecular dynamics. J. Chem Phy. 162(8): 084103

[16] Martyna, G. J., Tobias, D. J. & Klein, M. L. (1994). Constant pressure molecular dynamics algorithms. *The J. of Chem. Physics*, 101(5), 4177–4189. https://doi.org/10.1063/1.467468

[17] Joost, J.-P., Ludwig, P., Kählert, H., Arran, C. & Bonitz, M. (2014a). Screened coulomb potential in a flowing magnetized plasma. *Plasma Physics and Controlled Fusion*, 57(2), 025004. https://doi.org/10.1088/0741-3335/57/2/025004

[18] Frenkel, D. & Smit, B. (2023). *Understanding Molecular Simulation: From Algorithms to Applications*. Elsevier.

[19] Yukawa, H. (1935). On the interaction of elementary particles. I. *Proceedings of the Physico-Mathematical Society of Japan. 3rd Series*, 17, 48–57. https://doi.org/10.11429/ppmsj1919.17.0_48

[20] Zoppi, M. B. U. (1994). *Dynamics of the Liquid State|CiNii Research*. https://cir.nii.ac.jp/crid/1360863107709599744

Citing this Article

Abdullahi, A. D., Liman, M. S., Otto, M. S., Muhammad, F. U., Kamal, G., & Liman, Z. S. (2026). Molecular dynamics study of structural properties in a strongly coupled one-component plasma using LAMMPS. *Lafia Journal of Scientific and Industrial Research*, *4*(1), 157–167. https://doi.org/10.62050/ljsir2026.v4n1.782